Chapter 3

Model Predictive Control of Solar Cooling Plants: Review and Applications

Antonio J. Gallego, Adolfo J. Sánchez, Juan M. Escaño and Eduardo F. Camacho

3.1. Introduction

Currently, governments are promoting the use of renewable energy sources to reduce the environmental impact produced by the use of fossil fuels [8, 28]. Solar energy is, by far, the most abundant source of renewable energy. In fact, wind and most of the hydraulic energies come from solar energy [11, 16].

One important application of solar energy is the supply of air conditioning in buildings. The use of solar energy for air conditioning is spurred by the fact that high demands of air conditioning are required when high levels of solar radiation exist.

In this chapter a review of the state of the art, control algorithms and applications concerning solar energy plants (thermal and solar cooling) is presented. Two Model Predictive Control (MPC) algorithms developed for the solar cooling plant located at the Escuela Superior de Ingenieros at the Universidad de Sevilla are also described. These strategies show that the application of advanced control techniques to solar power plants can improve the operation of this kind of plants.

The chapter is organized as follows: Section 3.2 presents the state of the art of solar projects around the world, control objectives, and several advanced control approaches developed to control the temperature of this kind of plants. Section 3.3 describes the solar cooling plant used as a test-bench in this chapter. Section 3.4 presents the mathematical model

Antonio J. Gallego
Departamento de Ingeniería de Sistemas y Automática, Universidad de Sevilla, Spain

of the plant used to test the control algorithms. Section 3.5 presents an application of a MPC control algorithm used to regulate the outlet temperature of the Fresnel collector field around a desired set-point. Section 3.6 shows the development of an hybrid MPC control algorithm which chooses the operation mode in which the solar cooling plant work according to the environmental conditions and the state of the plant. Finally, Section 3.7 presents some concluding remarks.

3.2. State of the Art

One of the main applications of solar energy is producing electricity in solar thermal plants. A solar thermal plant is composed of a solar field which heats up a heat transfer fluid (usually synthetic oil) to a desired temperature, a steam generator which uses the heated fluid to produce electricity, a storage system which provides energy when the solar field is not capable of doing it, and auxiliary elements such as valves, pipes etc. [28].

Many examples of solar thermal plants can be found around the world. For instance, the three 50 MW Solaben and the two 50 MW Solacor parabolic trough plants of Atlantica Yield in Spain, and the SOLANA and Mojave Solar parabolic trough plant located at Arizona and California, each of 280 MW power production. PS10 (10 MW), PS20 (20 MW) and Khi Solar One are examples of solar tower plants operated by Atlantica Yield and Abengoa Solar respectively [26, 30].

Although most of the solar thermal plants uses parabolic trough or solar tower technologies, several plants using Fresnel technology for producing electricity exist around the world. For example the Fresnel solar plant located at Puerto Errado in Murcia (Spain) which produces 30 MW of electricity. Another important Fresnel solar plant is the one constructed in Dacheng Dunhuang (China) which produces 50 MW of electricity. This was connected to the grid on December 2019 and possesses a storage capacity of 15 hours [54]. Fresnel technology for solar thermal plants is quickly growing around the world due to its simplicity and low cost compared to parabolic trough. They use cheaper flat glass mirrors, which are a standard mass-produced commodity, and that they require less steel and concrete as the metal support structure is lighter which simplifies the assembly process and leads to cost reductions. The Fresnel technology is also incorporating storage systems [53].

Another important application of solar energy is the supply of air conditioning in buildings. This application benefits of the fact that the need of air conditioning is well correlated with high levels of solar radiation. [34, 55].

This chapter presents two control algorithms designed for the solar cooling plant located at the Engineering School (ESI) of Seville [6, 49]. This plant consists of a Fresnel collector field, a double effect LiBr+ water absorption chiller and a storage tank. The water chiller is powered by hot pressurized water coming from the Fresnel solar field at 140-170 °C and produces air conditioning. When the solar radiation levels are not sufficient for reaching the required temperatures, the storage tank can be used. If the water temperature reaching the high temperature generator of the absorption machine is below 135 °C, the absorption machine uses natural gas.

In general, the control aim in solar plants is keeping the outlet temperature of the solar field as close as possible to a desired temperature set-point [20]. Since the decade of 1980, a considerable effort has been done concerning the development of control algorithms for solar power plants. Many of them were designed and tested for the experimental solar parabolic trough plant of ACUREX at the plataforma solar de Almera [18]. In [14] and [15] a review of different control strategies applied to the ACUREX plant is presented. An adaptative control scheme which cancels the resonance modes of the distributed collector field is presented in [3]. In [22], an observer based MPC was developed and tested at the ACUREX field. In [4] a practical nonlinear MPC is designed. More recently, in [33] a nonlinear continuous-time generalized predictive control (GPC) applied to the distributed collector field ACUREX is presented and tested in simulation. In [17] and [36] different advanced control strategies using predictive and adaptative control strategies are described.

Concerning the control of Fresnel solar collector fields, the research effort developed has not been so wide. In [59] and [58] different control schemes for a Fresnel collector field are presented and an explicit model predictive controller is developed and tested in a simulation environment. In [60] a sliding model predictive control based on a feedforward compensation is developed and tested in simulation for a Fresnel collector field. In [23] a gain scheduling generalized predictive controller (GPC) is developed and tested at the real Fresnel plant described in this chapter. It showed a good performance when tracking

references and disturbances rejection. In [39], a linear Fresnel solar plant is modeled and some control strategies are proposed for this plant. The model was adjusted using data from test field of the Solar Living Lab of Consorzio ARCA in Palermo, Italy. More recently, in [25], an adaptative Model Predictive Control strategy (MPC) is developed for the Fresnel collector field located at the University of Seville. That strategy was tested on simulation and at the real plant showing a good performance in all tests.

In this chapter, an incremental observer-based model predictive control algorithm is developed [13]. The control strategy uses a linearization of the nonlinear distributed parameter model to obtain the linear models. The MPC algorithm uses an incremental formulation which ensures an offset-free response without using disturbance estimators as long as the reference is constant and reachable. Its performance is compared to that obtained with a gain scheduling GPC [23]. The proposed control strategy shows faster tracking references. Since only the inlet and outlet fluid temperatures are measurable, the intermediate temperatures as well as the metal temperatures have to be estimated. The MPC strategy uses a robust Luenberger estimator. The estimator gain is obtained by a robust pole-placement technique allowing the imposition of stability constraints. The resulting problem can be solved via Linear Matrix Inequalities (LMI) considering a polytopic uncertainty of the plant. The main problem when using nonlinear estimators such as the unscented Kalman filter (UKF) is that imposing performance requirements and proving stability is a very difficult issue [46] and [45]. Furthermore, the stability of the MPC+UKF control strategy is still an open problem.

Another important control issue arising when controlling solar cooling plants is the need of choosing the operation mode for the plant [40, 55, 61, 63]. The control approaches designed for this kind of plant have usually a twofold goal: a) regulating the outlet temperature of the solar collector field and b) choose the operation mode. Since the operation mode is defined by a set of valves positions (discrete variables), the overall control problem is a nonlinear optimization problem which involves discrete and continuous variables. This problems are difficult to solve within the normal sampling times for control purposes (around 20-30 seconds) [44].

This chapter presents a different approach published in [12]. The control strategy uses two independent algorithms. The first one is a nonlinear model predictive control (MPC) which regulates the outlet temperature

of the Fresnel collector field. The second algorithm, which decides the operation mode, is based on a fuzzy logic to decide in which operation mode the plant has to work.

The following abbreviations are used in this chapter:

MPC	Model Predictive Controller;
GPC	Generalized Predictive Control;
GS-GPC	Gain-Scheduling Generalized Predictive Controller;
UKF	Unscented Kalman Filter;
PCM	Phase Change Material;
PDE	Partial differential equations;
FIS	Fuzzy Inference System.

3.3. Plant Description

The solar cooling plant consists of three subsystems: the double-effect LiBr+ water absorption chiller of 174 kW nominal cooling capacity. The solar Fresnel collector field heats up the pressurized water and delivers it to the water absorption chiller. If the solar field cannot reach the required temperature for the absorption machine operation, the PCM storage tank can be used. Fig. 3.1 shows the scheme of the whole plant.

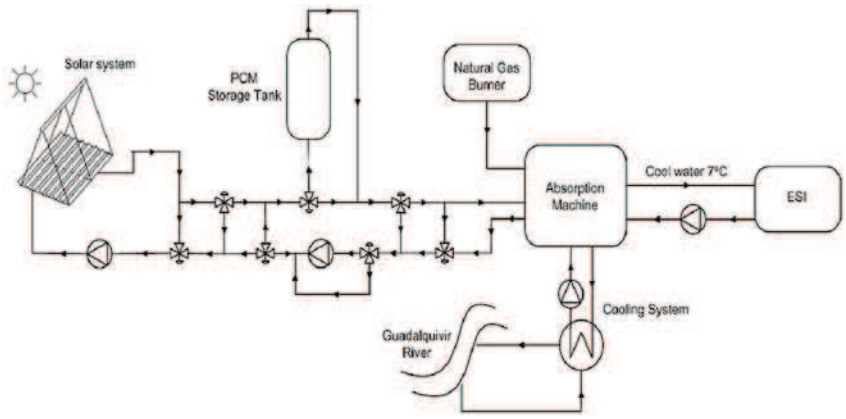

Fig. 3.1. Plant general scheme.

Water absorption chiller: this is a double-effect cycle LiBr+ absorption machine with 174 kW and a theoretical COP of 1.34. It transforms the thermal energy (hot water at 140-170 °C) coming from the Fresnel solar field or the Phase change material (PCM) storage tank, into cold water to be used by the ESI of Seville [6]. Apart from the hot water, a cooling fluid for the condenser is needed in the absorption machine. This is obtained from the water catchment of the Guadalquivir river.

Solar Field: the solar field consists of a set of Fresnel solar collectors (see Fig. 3.2) which concentrate the direct solar radiation onto the receiver tube placed in a plane parallel to the solar field. The metal tube is enveloped by a thin metal case called the secondary reflector. The secondary reflector aims at reflecting the solar beams which do not have direct impact on the receiver. The energy collected by the receiver tube is then transferred to a heat transfer fluid (in our case, pressurized water).

Fig. 3.2. Fresnel collector field.

The solar field orientation is East-West, and the sun-tracking system modifies the inclination of every row to concentrate the sun beam onto the metal tube. To do this, the sun-tracking system computes the solar vector by using the well known formulas for solar azimut and solar height [28], and then calculates the desired inclination of every row using the relative position between the row and the tube as explained in [49].

To change the flow provided by the water pumps, the pump speed variation has to be used. Since the control signal provided by the control algorithm proposed here is the water flow, an intermediate PID controller is used. It receives the water flow set-point and modifies the speed variator accordingly to obtain it.

PCM storage tank: The PCM storage is a tank of 18 m long and 1.31 m of diameter (Fig. 3.3). The storage tank is a shell-tube heat exchanger with a theoretical thermal storage capacity of 275.5 kWh (145-180 °C) and 150 kW. It consists of a series of tubes containing a heat transfer fluid and the PCM fills up the space between tubes and the shell. The theoretical thermal storage is computed by using the properties of the hydroquinone. the total mass of the PCM is of 3294 kg [51]. The melting temperature of the hydroquinone is about 170 °C which is suitable for the water absorption chiller operating range [24].

Fig. 3.3. PCM storage tank.

3.4. Modelling of the Plant Subsystems

In this section, the model of each subsystem comprising the whole plant is described. The solar cooling plant has four subsystems: the Fresnel solar field, the storage tank, the absorption machine and the piping system connecting them. The equations governing the dynamics of each subsystem are presented. The models are validated and compared to real data taken from the plant.

Since the main goal of these models is to be used in control algorithms, the balance equations of each subsystem should be as simple as possible and an adequate trade-off between precision and complexity is indispensable.

3.4.1. Fresnel Solar Field

In this subsection, the mathematical model of the Fresnel collector field is presented. Two approaches are usually considered in this kind of

systems: the lumped parameter model (developed in [49]) and the distributed parameter model (described in [56]). In this chapter, a distributed parameter model has been used. The distributed parameter model is governed by the following two partial derivative equations (PDE) ([9, 21]):

$$\rho_m C_m A_m \frac{\partial T_m}{\partial t} = IK_{opt} noG - H_l G(T_m - T_a) - LH_t(T_m - T_f), \quad (3.1)$$

$$\rho_f C_f A_f \frac{\partial T_f}{\partial t} + \rho_f C_f q \frac{\partial T_f}{\partial x} = LH_t(T_m - T_f), \quad (3.2)$$

where m subindex refers to metal and f subindex refers to a fluid. In Table 3.1, parameters and their units are shown. The same system of equations is used to model the piping system. In this case, the radiation reaching the tube is nil and the thermal losses coefficient takes a different value.

Table 3.1. Parameters description.

Symbol	Description	Units
t	Time	s
x	Space	m
ρ	Density	kgm^{-3}
C	Specific heat capacity	$JK^{-1}kg^{-1}$
A	Cross sectional area	m^2
$T(x, y)$	Temperature	K, C^{-1}
$q(t)$	Oil flow rate	$m^3 s^{-1}$
$I(t)$	Solar radiation	Wm^{-2}
no	Geometric efficiency	Unitless
K_{opt}	Optical efficiency	Unitless
G	Collector aperture	m
$T_a(t)$	Ambient temperature	K, C
H_l	Global coefficient of thermal loss	Wm^{-2} C^{-1}
H_t	Coefficient of heat transmission metal-fluid	Wm^{-2} C^{-1}
L	Length of pipe line	m

The PDE system is solved by dividing the metal and fluid in 64 segments of 1 m long. The integration step is chosen of 0.5 seconds.

As has been mentioned before, the heat transfer fluid is pressurized water whose density and specific heat have been obtained as polynomial functions of the segment temperature using thermodynamical data of pressurized water. The heat transfer coefficient depends on the segment temperature and the water flow [35]. As far as the thermal losses coefficient is concerned, it was obtained using experimental data from the collector field [49] and [23]. Figs. 3.4 and 3.5 show a comparison between the model and the real plant evolution. The model evolution behavior is very similar to the real solar field as can be seen.

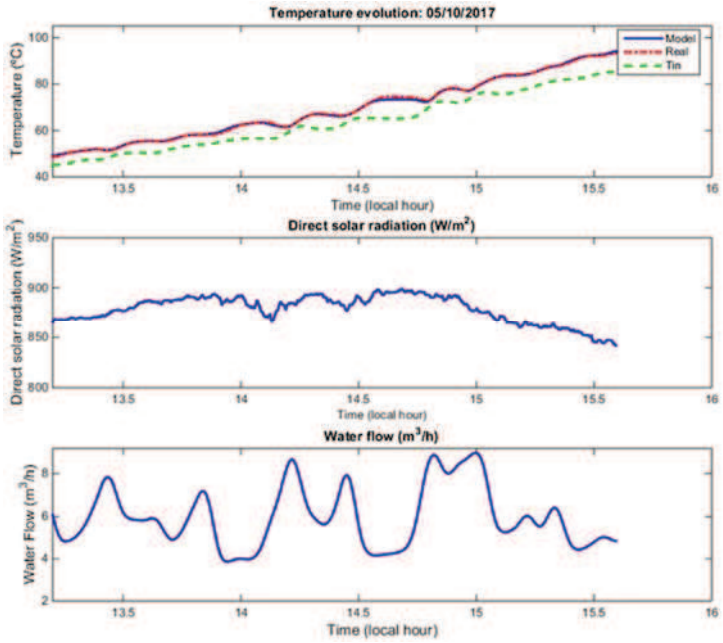

Fig. 3.4. Solar field evolution Model vs Real: 05/10/2017.

3.4.2. PCM Storage Tank

In order to model the storage tank dynamics, two stages are considered: when the PCM is in the sensible heat transmission state, the PCM behavior is modeled by a double-capacity model. In the phase change

stage, the solution is based on the Stephan solution. In [51], a more complete description of the PCM storage tank is carried out. The subsection provides a brief description of the model. The model was published in [24].

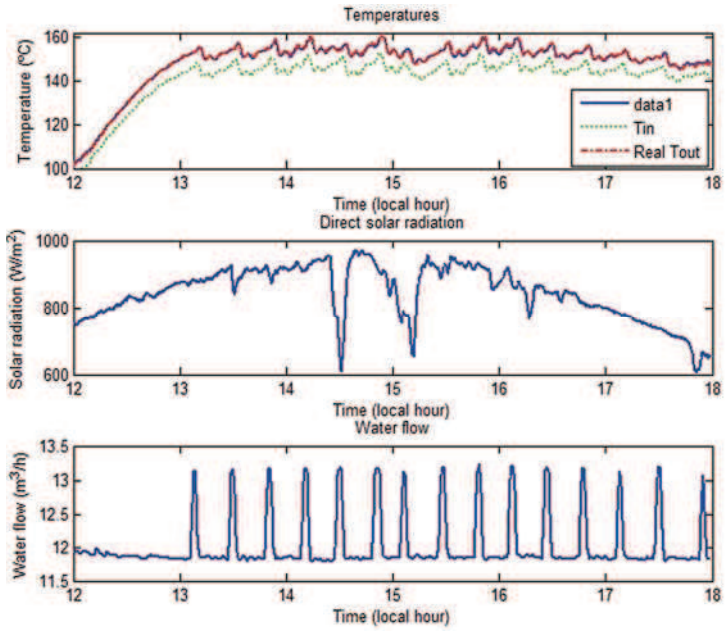

Fig. 3.5. Solar field evolution Model vs Real: 29/06/2009.

Double Capacity Model

In this stage, the model consists of two different capacitive zones, with a thermal resistance between both of them. The r_e and r_i radius denote exterior and interior radius respectively, r_m is the separation radius between the two capacities zones, which is a parameter that has to be identified. T_1 and T_2 represent temperatures of zones 1 and 2, h is the convective heat transfer coefficient, K the conductivity, C_p the specific heat and T_∞ stands for the hot water temperature [51].

The model has two differential equations, one per zone:

$Zone 1$:

$$\pi\ \rho C_p(r_m^2 - r_i^2)\frac{dT_1}{dt} = 2h\ \pi r_i(T_\infty - T_1)$$

$$-\frac{2\pi K(T_1 - T_2)}{ln(r_e / ri)} \tag{3.3}$$

$Zone 2$:

$$\frac{2\pi K(T_1 - T_2)}{ln(r_e / ri)} = \rho C_p \pi(r_e^2 - r_m)\frac{dT_2}{dt} \tag{3.4}$$

The aforementioned equations are valid for the liquid and solid phase. However, parameters such as the conductivity K and the density of the hydroquinone ρ may have different values.

Stefan Solution for Phase Change

When the PCM reaches a temperature of 170 °C, the hydroquinone reaches the melting point and the phase change stage starts. To model this stage, the liquid and solid phases are considered to be stable. The dynamics of the hydroquinone temperature is governed by the Stefan solution. This solution establishes an inferior limit of stored energy in a phase change phenomenon as well as a velocity limit for its evolution. Since the Stefan number given by the expression (3.5) is very small finding a solution supposing a semi-infinite medium and that all the material is initially at the phase change temperature is possible [38] and [42].

$$S_T = \frac{C_p(T_f - T(r_i))}{L} \tag{3.5}$$

The final expressions of the Stefan solution are given by equations (3.6) and (3.7):

$$T(r) = T_f + \frac{h\,r_i}{K}\left(\frac{T_f - T_\infty \dfrac{h\,r_i}{K} ln(r_i / R)}{1 - \dfrac{h\,r_i}{K} ln(r_i / R)} - T_\infty\right) ln(r / R),$$

$$t_{st} = C\left(r_i\left[\frac{r_i h}{K} - 2\right] - R^2\left(\frac{2h}{K} ln(r_i / R) + \frac{h}{K} - \frac{2}{r_i}\right)\right), \tag{3.6}$$

$$C = \frac{\rho L^*}{4h(T_\infty - T_f)}, \tag{3.7}$$

where $R = R(t_{st})$ is the interface position which depends on t_{st} (Stefan time), T_f is the melting temperature, $T(r)$ is the PCM temperature which depends on the radius and L^* is the corrected latent heat of hydroquinone. In [51] and [24], all the modeling details and parameters estimation are better explained.

Fig. 3.6 shows a comparison between the model and the real temperature of the storage tank evolution. At time 14.45 h the inlet valve opens and the hot water heats up the storage tank. As can be observed, the model matches well the real data with a maximum error of a 2.5 %.

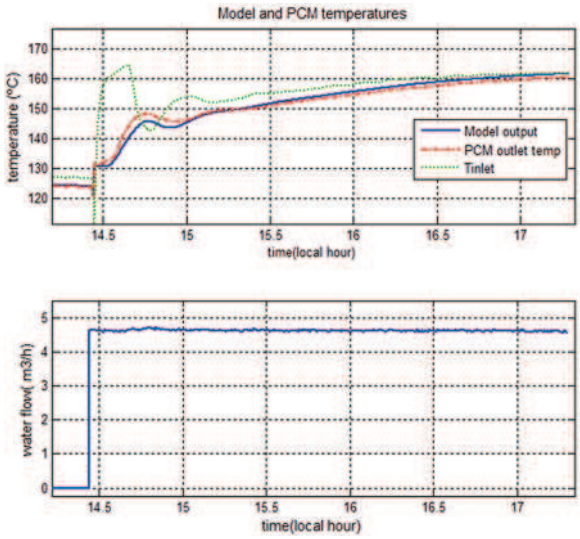

Fig. 3.6. PCM temperature evolution: Model vs Real.

3.4.3. Absorption Machine Model

The absorption machine is formed by three different elements: a high temperature generator, a refrigeration system and an evaporator [32, 47]. Several approaches to model these kind of systems can be found in literature.

These approaches go from complex thermodynamics models such as the model proposed in [29]. These approaches are too complicated to be used for control purposes. The model proposed in this chapter is a simple model: each subsystem is modeled as a grey box model. The dynamics is modeled by a lumped parameter model with constant heat capacities and the model coefficients were identified using data from the real water chiller [12].

Figs. 3.7 and 3.8 show a comparison between the model and the real water chiller evolution. As can be seen, the model evolution is similar to the real system evolutions in spite of the simplifications considered.

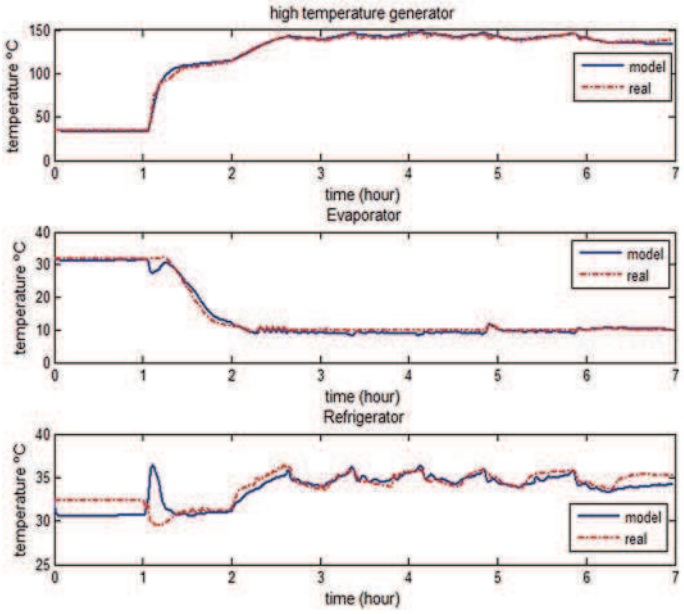

Fig. 3.7. Absorption machine model vs Real: 19/07/2010.

High Temperature Generator

The energy balance equation describing the output temperature of the generator is given by equation (3.8):

$$C_g \frac{dT_{ogen}}{dt} = Q_{cald} - Q_{gloss} + \rho_w \, q_h C_w (T_{ogen} - T_{igen}), \qquad (3.8)$$

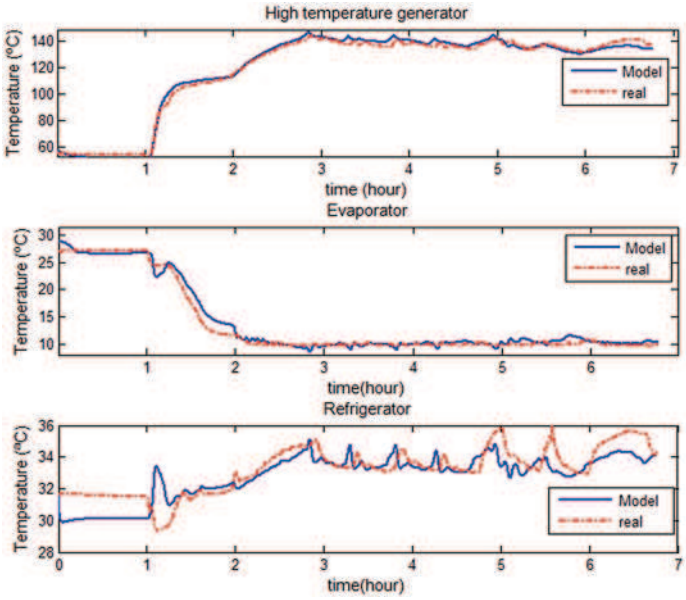

Fig. 3.8. Absorption machine model vs Real: 21/07/2010.

where T_{ogen} and T_{igen} represent the outlet and the inlet temperature of the high temperature generator, Q_{cald} is the thermal power supplied by the absorption machine burner (W), Q_{gloss} are the thermal losses (W), C_g is the generator heat capacity, ρ_w and C_w are the density and the specific heat of the water, and q_h is the generator water flow.

Evaporator

The energy balance equation describing the output temperature of the evaporator is given by equation (3.9):

$$C_{ev}\frac{dT_{oevap}}{dt} = -Q_{ev} - Q_{ev_loss} + \rho_w\, q_{ev} C_w (T_{iev} - T_{oev}), \qquad (3.9)$$

where T_{oev} and T_{iev} represent the outlet and the inlet temperature of the evaporator, Q_{ev} is the cooling power supplied by the absorption machine (W), Q_{ev_loss} are the thermal losses (W), C_{ev} is the evaporator heat capacity, q_{ev} is the evaporator water flow.

Refrigerator

The energy balance equation describing the output temperature of the Refrigerator is given by equation (3.10):

$$C_{refr}\frac{dT_{orefr}}{dt} = Q_{refr} - Q_{refr_{loss}} + \rho_w\, q_{ref} C_w (T_{irefr} - T_{orefr}), \quad (3.10)$$

where T_{orefr} and T_{irefr} represent the outlet and the inlet temperature of the refrigerator, Q_{refr} is the thermal power dissipated by the refrigerator (W), $Q_{refr_{loss}}$ are the thermal losses (W), C_{refr} is the refrigerator heat capacity, q_{ref} is the refrigerator water flow.

The next section is devoted to show an MPC-based control algorithm for the solar field which had a good performance.

3.5. Model Predictive Control Algorithm for the Fresnel Solar Collector Field

In this section a brief review of several control algorithms applied to the Fresnel collector field is conducted. Then, a Model Predictive Control algorithm used to regulate the outlet temperature of the solar field is presented. This algorithm was published in [13].

The control objective in a solar energy plant is to maintain the outlet temperature of the solar field around a desired set-point [9]. The water flow is used to accomplish this task. The objective is not an easy matter for two reasons:

• The system dynamics is complex and highly nonlinear particularly at low water flows. The input-output delay changes substantially with respect to the flow. This point increases the difficulty of the temperature control at low flows.

• A solar power plant is affected by multiple disturbance sources: inlet temperature, ambient temperature, solar time, solar radiation etc. The solar radiation is the most important one and can change very abruptly throughout the operation (for example when passing clouds are affecting the solar field) [52].

The algorithm was tested on a nonlinear model showing better performance compared to other control strategies. Furthermore, a test carried out at the real plant was performed. The controller showed a good behavior in both cases. Good tracking capabilities and fast responses were obtained without great oscillations.

Model Predictive control strategies have demonstrated to be one of the most efficient control techniques when dealing with the control solar energy plants [17]. Many MPC control strategies have been applied to solar power plants, in particular to the old ACUREX solar collector field at the Plataforma Solar de Almera (PSA). For example in [4] a practical nonlinear MPC is developed. In [33] a nonlinear continuous time generalized predictive control (GPC) is developed and tested by simulation. In [2], an improvement of a Gain Scheduling Model Predictive controller is proposed and tested on a model of the ACUREX solar field. These are examples of recent works concerning the control of the ACUREX solar trough field.

As far as the application of control strategies for Fresnel solar collector field, some examples can be given. In [58], examples of control approaches for Fresnel collector field are presented and discussed. An explicit model predictive control strategy is tested on a nonlinear model of the plant. In [60] a sliding model predictive control based on a feedforward compensation is developed for a Fresnel collector field and tested on a nonlinear model of a Fresnel collector field. In [5], control systems for direct steam generation in linear concentrating power plants are investigated. In [41], control laws for linear Fresnel plants have been developed. More recently, in [23] a Gain Scheduling Generalized Predictive Controller was developed and tested for a Fresnel collector field. In [25] an adaptative MPC control strategies which uses an unscented Kalman filter [57] for estimating both the metal-fluid temperature profiled and the effective solar radiation, was tested at the real plant with good results. The controller showed that controlling these kind of plant without a measurement of solar radiation is possible.

The set MPC+UKF has been widely used in the control of solar energy system. The models describing the dynamics of a Fresnel collector field are complex and nonlinear due to the highly nonlinear dynamics of these kind of systems [20]. More recent examples can be found in [27] where a neural model-based MPC strategy using an UKF for estimating the weights and biases was tested at the real ACUREX solar field. In [31], an iterative extended Kalman filter is used to estimate the states and solar

radiation for control purposes. The estimator was used in conjunction with a controller tested on a simulator of the Shiraz solar plant.

The main advantage of using the UKF as a state estimator is that a nonlinear model can be used and no linearization and computation of the Jacobian matrix are needed [37, 64]. The main disadvantage is that proving stability and the imposition of the dynamics constraints for the estimator is a difficult task. Using other strategies allows to impose dynamics behavior for the state observer [22].

In this section, an incremental offset-free state-space Model Predictive Controller (MPC) is described for the Fresnel collector field located at the solar cooling plant installed on the roof of the Engineering School of Sevilla. A robust Luenberger observer was used for estimating the non-measurable states. The proposed strategy was tested on a nonlinear distributed parameter model of the solar field and compared to the performance of a Gain-Scheduling Generalized Model Predictive Controller (GS-GPC). A faster reference tracking was obtained. Moreover, a real test was carried out at the real plant. This test showed that the proposed strategy achieved a very good performance [13].

3.5.1. Incremental Model Predictive Control Strategy

In this section, the observer-based state-space MPC is presented. Basically, a MPC control algorithms consists of the following 3 steps [10, 48]:

1. Use a model to predict the process evolution at future time instants (horizon), depending on a control sequence;

2. Compute the control sequence which minimizes a certain objective function;

3. Apply only the first element of the control sequence, then in the rest of sampling instants recalculate the sequence shifting the horizon one step in the future (receding horizon). Repeat steps 1 to 3.

In general, the mathematical expression of the MPC problem can be posed as follows:

$$\min_{\Delta u} J = \sum_{t=1}^{N_p} \left(y_{k+t|k} - y_{k+t}^{ref} \right) \left(y_{k+t|k} - y_{k+t}^{ref} \right) + R_u \sum_{t=0}^{N_c-1} \Delta u_{k+t|k} \Delta u_{k+t|k}, \quad (3.11)$$

s.t.

$$y_{k+t|k} = f(\Delta u, y_{k+t-1}, y_{k+t-2}, ...),$$
$$u_{k+t|k} = u_{k+t-1|k} + \Delta u_{k+t|k},\ u_{\min} \le u_{k+t|k} \le u_{\max},\ t = 0, \quad , N_p - 1 \qquad (3.12)$$

The use of a conventional linear models (as is the case here) to predict the evolution of the outlet temperature in a plant with highly nonlinear dynamics presents some drawbacks. The performance of linear controllers deteriorates when the plant evolves far from the linearization point. This problem becomes more evident at low water flows as stated [7].

In order to overcome this drawback, in this chapter the linear model is computed each sampling time. The sampling time is chosen as 20 seconds. the state-space matrices used by the MPC are obtained by linearizing the nonlinear distributed parameter model (3.2). The metal tube is divided into 4 segments. Thus, there are 8 states: 4 for the metal temperature and 4 for the fluid temperature. This simplification reduces significantly the complexity and the computational burden of the control strategy. The drawback of this approach is the loss of precision.

Only the inlet and the outlet temperature of the fluid are available, the temperatures of metal segments and fluid in the intermediate sections have to be estimated. The state estimator is a robust Luenberger state-observer. The observer gain is computed using a robust pole-placement via LMI considering a polytopic uncertainty of the plant dynamic [19]. Using this approach, the stability of the state observer is ensured by imposing stability and performance conditions to the closed loop poles in the z plane [1].

The final control scheme is presented in Fig. 3.9. Every 20 seconds the data acquisition system takes the data from the field and the state observer computes the estimated states. This estimation is provided to the block which computes the linear matrices and solves the MPC problem given by equation (3.12). The MPC optimizer computes a control signal, q , which is applied to the Fresnel collector field. Fig. 3.9 shows this control scheme.

Fig. 3.10 shows the first simulation consisting of a series of changing set-points for the outlet temperature. The direct solar radiation corresponds to a clear day with passing clouds. The data to carry out the

simulation corresponds to the day 29 June of 2009. The temperature reference is initially at 120 °C.

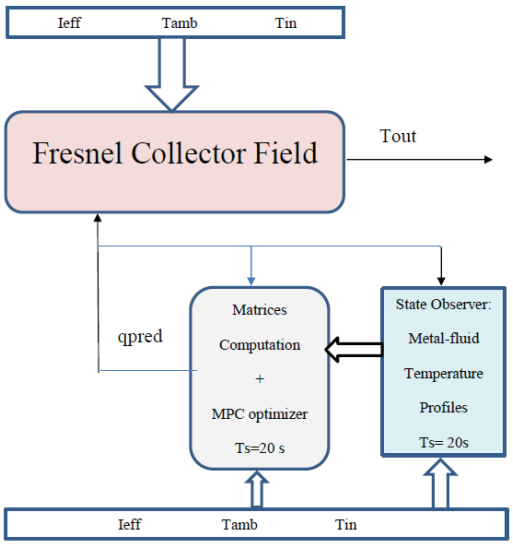

Fig. 3.9. Final Control Scheme.

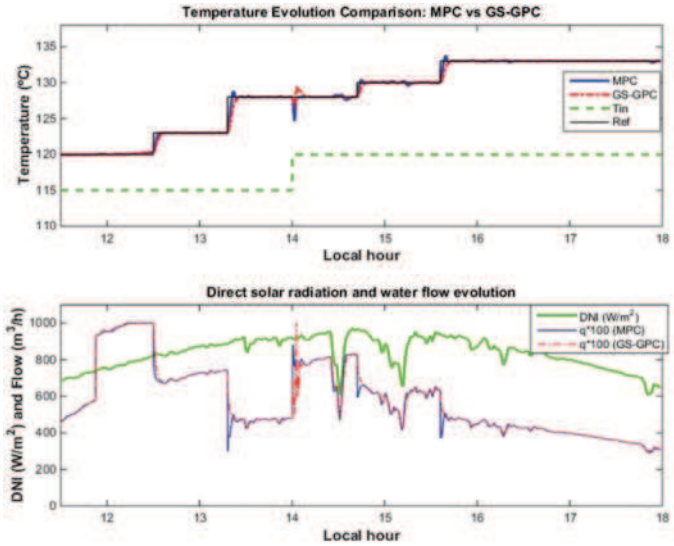

Fig. 3.10. Simulation 1: Tracking references.

As can be seen, the MPC controller provides faster responses with very small overshoots. Both controllers reject properly the disturbances in the solar radiation and the inlet temperature.

Table 3.2 shows the comparison of the ITAE and ISE criteria for both controllers. The MPC control strategy outperforms the GS-GPC control strategy as observed.

Table 3.2. Simulation 1: Performance comparison using ITAE and ISE criteria for the comparison between the GS-GPC and the MPC.

ITAE Criterion	GS-GPC	MPC
	3715.2	2612.4
ISE Criterion	GS-GPC	MPC
	751.95	400.351

Fig. 3.11 depicts the comparison between the temperature profiles obtained by the robust Luenberger observer and those provided by the distributed parameter model.

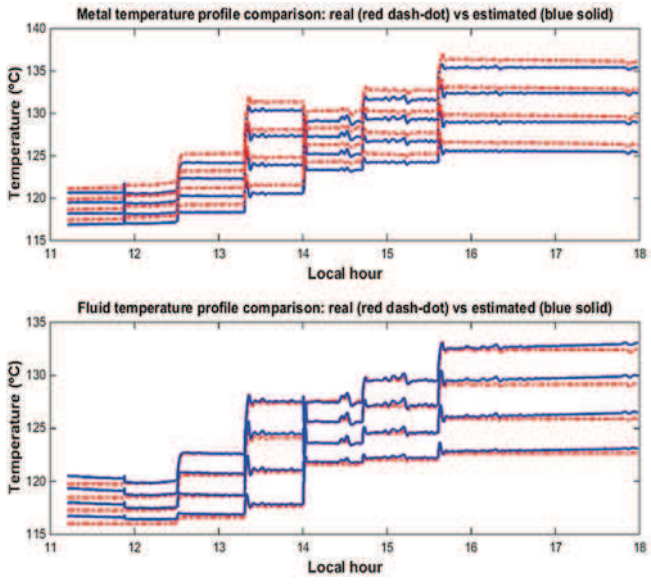

Fig. 3.11. Simulation 1: Temperature profiles estimation. Estimated (solid blue line) and Distributed parameter model (dash red line).

The estimated profiles tracks well the real measurements with small steady-state errors. These errors are produced by using a lower number of segments in the linear model than that used for the full nonlinear model. In spite of this fact, the maximum error observed is about 1 °C.

The real test carried out on 22/10/2017 at the real Fresnel collector field is presented in Fig. 3.12. The plant was working in recirculation mode. In this mdoe the outlet temperature of the solar field is recirculated through a long pipe and returns to the solar field. In this mode the plant is constantly affected by inlet temperature disturbances. The inlet temperature disturbances are difficult to reject because its associated residence time depends on the water flow [50]. The allowed flow range is confined to 3.7-9 m^3 / h .

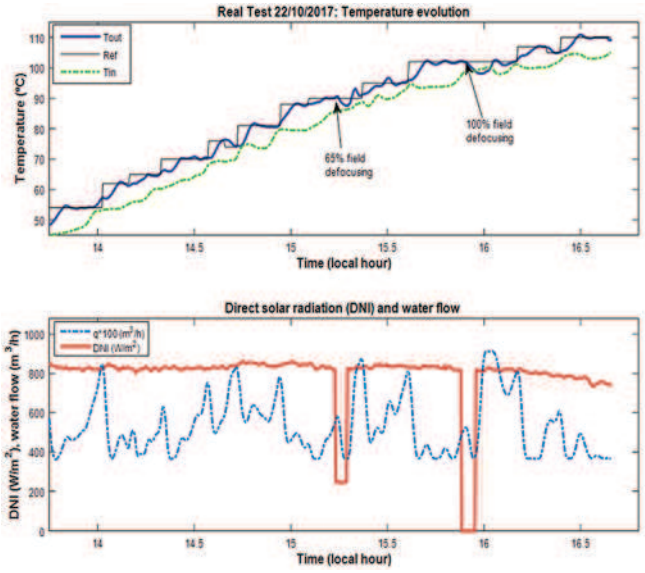

Fig. 3.12. Real Test carried out on 22/10/2017.

From the beginning to 15 h, the test consisted of a series of changing references which the controller tracks well as seen in Fig. 3.12. The rise times obtained were around 4-6 minutes. As can be seen, the controller achieves an offset-free tracking. At 15.2 h the 65 % of the mirrors were defocused for 3 minutes to simulate a passing cloud. As seen, the controller recovers the temperature after an overshoot of 3.5 °C and

steers the outlet temperature to the desired set-point. At 15.9 h, the solar field is completely defocused for 4 minutes. Since the controller cannot track the set-point, the water flow is reduced to the minimum value. When the solar field is focused again, the controller tracks the desired set-point with small overshoots. After that, the controller tracks properly the temperature set-points.

3.6. Hybrid Control of the Solar Cooling Plant

As mentioned above, solar cooling plants can work in different operation modes so that the plant can be considered a hybrid system. The control approaches for this kind of systems has to fulfill two goals: a) regulating the outlet temperature of the solar collector field around a desired set-point and b) select the adequate operation mode [62].

An operation mode is defined by the position of the valves positions (discrete variables). The overall control problem is a nonlinear optimization problem involving discrete and continuous variables. This kind of problems are usually very difficult to solve within the sampling time for control purposes (20-30 seconds) [43].

Several approaches have been used to address these kind of problems. For example, choosing the operation mode using a series of rules established by expert operators [63, 55, 40].

In this section, a two layer control strategy is proposed. The first layer is a nonlinear model predictive controller for regulating the outlet temperature of the solar field. The second layer is a fuzzy algorithm which selects the adequate operation mode for the plant taken into account the operation conditions. The control strategy is tested on a model of the plant showing a proper performance [12].

The proposed algorithm was tested on a nonlinear model of the plant using the Matlab simulation environment.

3.6.1. Hybrid MPC Control Strategy

The first layer of the control algorithm is the temperature regulator. The algorithm chosen to accomplish this issue is a nonlinear model predictive control. The general problem formulation can be posed using the problem (3.12) with the difference that the mathematical model used to

predict the future evolution of the outlet temperature is nonlinear. The resulting control problem is a nonlinear model predictive control problem.

The non-measurable states are estimated using an unscented Kalman filter.

As far as the modes selection is concerned, it is done by means of a fuzzy algorithm. A particular operation mode can be defined as a particular configuration of the subsystems, valves and pumps which compose the plant (Fig. 3.1). The choice of working in a particular operation mode is determined by the cooling demand, the state of the plant and weather conditions.

The algorithm was tuned in order to fulfill two conditions: a) transitions between operation modes have to be smooth, that is, fast commutations between modes are not allowed and b) only feasible transitions between the modes are possible. Those transitions are imposed as a constraints and have been designed by the experience of the plant operators.

The operation modes are listed and briefly described below:

- Mode 0: the solar field charges the PCM storage tank. There is no cooling demand and the water chiller is off;
- Mode 1: the solar field is connected to the absorption machine through the PCM tank. This mode is useful in two situations: the storage tank can provide energy if the solar field is not able to heat the water up to the required temperature for powering the chiller. The second situation occurs when there is an excess of solar radiation: the solar field can feed the absorption machine and load the PCM tank;
- Mode 2: The PCM storage tank powers the water chiller while the solar field is heated up by recirculating water;
- Mode 3: The tank is used for heating up the piping system. It can be useful early in the morning for a quick start-up;
- Mode 4: The tank supplies hot water to the water chiller if solar collectors cannot work. For instance, in a cloudy day when solar radiation is nil and the storage tank is charged;
- Mode 5: The water chiller is powered only by the solar collectors;

- Mode 6: Water is recirculated in the solar field circuit. The absorption machine uses natural gas.

Not all transitions among operation modes are allowed. Table 3.3 shows the possible transitions.

Table 3.3. Allowed transitions between operation modes.

Current \ Target	M.0	M.1	M.2	M.5	M.6
M.0	X	X	T_{0-2}	T_{0-5}	T_{0-6}
M.1	T_{1-0}	X	T_{1-2}	T_{1-5}	X
M.2	T_{2-0}	T_{2-1}	X	X	T_{2-6}
M.5	T_{5-0}	T_{5-1}	X	X	T_{5-6}
M.6	T_{6-0}	T_{6-1}	X	T_{6-5}	X

The transitions depend on the plant variables: outlet temperature of the solar field, energy stored in the PCM tank, cooling demand, environmental conditions etc.

Several points are worth pointing out:

- The minimum inlet temperature allowed for correct operation is about 135 °C. This should be taken into account because thermal losses exist in the pipe connecting the solar field to the water chiller.
- The storage tank can proportionate energy for 1 hour approximately when it is fully charged. The storage tank should be used only in the case when the amount of stored energy is high or the solar field is able to charge it.
- When solar radiation is high and the solar field is able to charge the storage tank and power the absorption machine, it should be done only if the temperature of the tank is high enough to ensure that the inlet temperature of the absorption machine is adequate for correct operation. For instance, if the outlet temperature of the solar field is 160 °C and the tank temperature is 120 °C, the use of mode 1 is not correct, because the temperature of the tank is smaller than that required for the absorption machine.

- The maximum absolute difference between the outlet temperature of the solar field and the storage tank temperature must be inferior to 30 °C, if the storage tank is to be used.
- In order to avoid very fast commutations of the modes, the fuzzy algorithm computes the adequate operation mode every 120 seconds.

In [12] the complete procedure is explained.

3.6.2. Simulation Results

In this section, simulations testing the hybrid algorithm proposed in the previous section are presented. The data corresponding to solar radiation was taken from the real solar field.

Fig. 3.13 shows a clear day where the storage tank had a temperature about 110 °C.

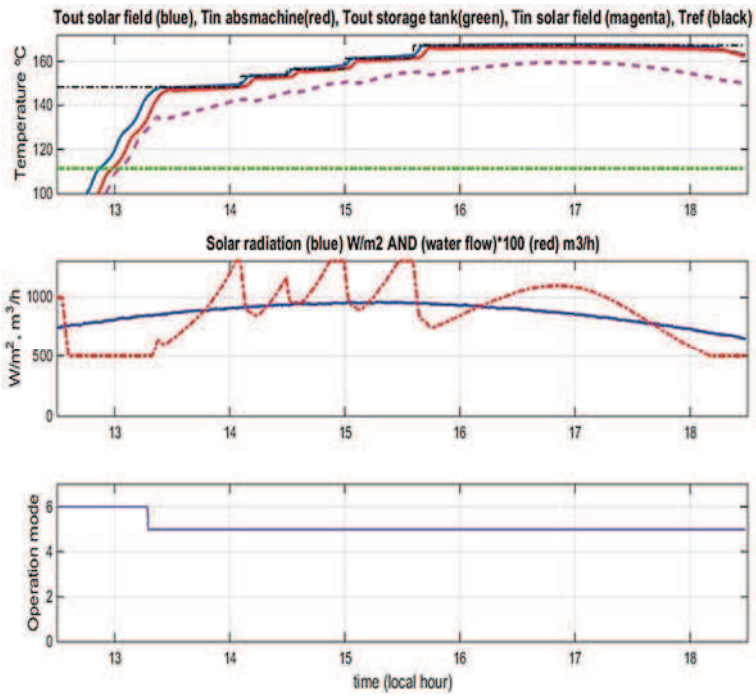

Fig. 3.13. Operation modes in a clear day.

The initial operation mode is mode 6 in order to recirculate and heat up the water. The initial temperature reference is about 145 °C. Once the outlet temperature of the solar field reaches an adequate value to feed the absorption machine (higher than 135 °C), the fuzzy algorithm commutes to mode 5, where the solar field is able to power the absorption machine. From 14 h onwards, the temperature reference consists of a series of increasing steps. As can be seen, the temperature regulator tracks properly these references. This is the normal operation in clear days, where the solar field is sufficient to power the water chiller.

Fig. 3.14 depicts the results of a day where some clouds affect the solar field. From 12.5 h to 12.9 h approximately, the solar field is in recirculation mode (mode 6) accumulation energy and increasing the outlet temperature. The reference temperature for the outlet temperature is 10 °C above the inlet temperature. This is done to maintain an approximately constant thermal jump without decreasing much the water flow. As can be seen the MPC controller tracks the reference properly in spite of the radiation disturbances.

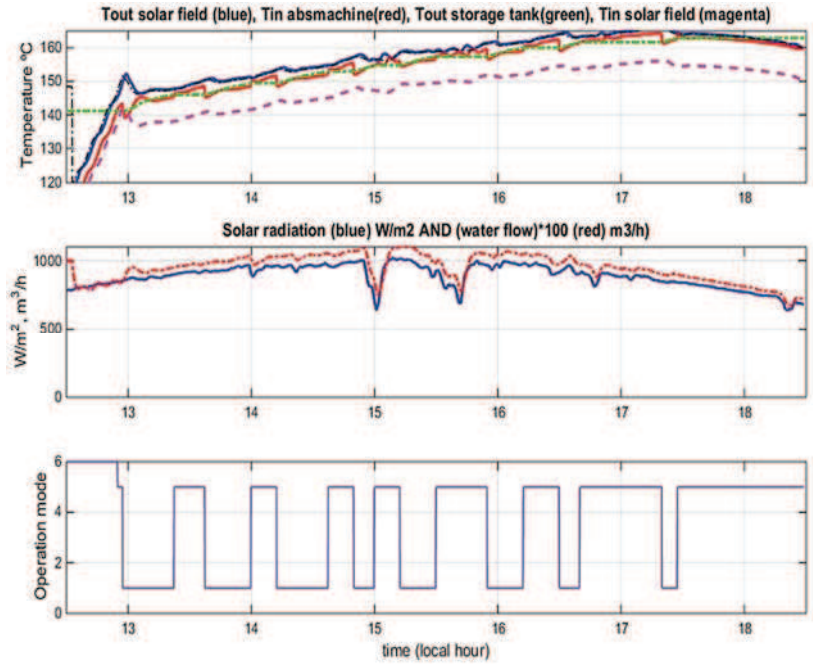

Fig. 3.14. Operation modes in a clear day: storage tank charging.

At 12.9 h the outlet temperature reaches a value higher than 135 °C and the fuzzy algorithm commutes to mode 5. At 12.95 h the solar field reaches a temperature about 150 °C which makes possible not only powering the water chiller but also accumulating energy in the storage tank. From 12.95 h onwards, the outlet temperature of the solar field is increased and the storage tank is charged (dashed green line). The fuzzy algorithm commutes between modes 5 and 1 depending on if the outlet temperature of the solar field and the storage temperature are close enough or not (approximately 4 °C). The main reason to do this is that, the temperature reaching the PCM tank is about 4 °C lesser than the outlet temperature of the solar field due to the thermal losses in the pipe. Only when the outlet temperature of the solar field is higher than 4 °C than that of the storage tank, it makes sense charging it.

3.7. Conclusions

In this chapter, an overview of the state of art concerning the control strategies developed for solar thermal plants has been presented. In particular a brief review of the control strategies for solar cooling plans has been conducted.

The mathematical model of the solar cooling plant located at the University of Sevilla has been described and two model predictive control algorithm have been shown. These two applications showed the importance of the applications of advanced control techniques for improving the operation of solar thermal plants. In particular, the hybrid model predictive control algorithm developed a way of choosing the operation mode using a fuzzy method which can alleviate the operator task concerning the choice of the operation mode. This can be a very difficult task since many variables have to be taken into account.

Acknowledgments

The authors would like to acknowledge the European Research Council for funding this work under Advanced Research Grant OCONTSOLAR (789051).

References

[1]. C. Afri, V. Andrieu, L. Bako, P. Dufour, State and parameter estimation: A nonlinear Luenberger observer approach, *IEEE Transactions on Automatic Control*, Vol. 62, Issue 2, 2017, pp. 973-980.

[2]. A. Alsharkawi, J. A. Rossiter, Towards an improved gain scheduling predictive control strategy for a solar thermal power plant, *IET Control Theory & Applications*, Vol. 11, Issue 12, 2017, pp. 1938-1947.

[3]. J. D. Álvarez, R. Costa-Castelló, M. Berenguel, L. J. Yebra, A repetitive control scheme for distributed solar collector field, *International Journal of Control*, Vol. 83, Issue 5, 2010, pp. 970-982.

[4]. G. A. Andrade, D. J. Pagano, J. D. Álvarez, M. Berenguel, A practical NMPC with robustness of stability applied to distributed solar power plants, *Solar Energy*, Vol. 92, 2013, pp. 106-122.

[5]. A. Aurousseau, V. Vuillerme, J.-J. Bezian, Control systems for direct steam generation in linear concentrating solar power plants: A review, *Renewable and sustainable Energy Reviews*, Vol. 56, 2016, pp. 611-630.

[6]. P. Bermejo, F. J. Pino, F. Rosa, Solar absorption cooling plant in Seville, *Solar Energy*, Vol. 84, 2010, pp. 1503-1512.

[7]. L. Brus, T. Wigren, D. Zambrano, Feedforward model predictive control of a non-linear solar collector plant with varying delays, *IET Journal of Control Theory and Applications*, Vol. 4, Issue 8, 2010, pp. 1421-1435.

[8]. E. F. Camacho, M. Berenguel, Control of solar energy systems, in *Proceedings of the 8th IFAC Symposium on Advanced Control of Chemical Processes*, Singapore, 2012, pp. 848-855.

[9]. E. F. Camacho, M. Berenguel, F. R. Rubio, Advanced Control of Solar Plants, *Springer Verlag*, London, 1997.

[10]. E. F. Camacho, C. Bordons, Model Predictive Control, 2nd Ed., *Springer Verlag*, 2004.

[11]. E. F. Camacho, A. J. Gallego, Optimal operation in solar trough plants: A case study, *Solar Energy*, Vol. 95, 2013, pp. 106-117.

[12]. E. F. Camacho, A. J. Gallego, J. M. Escano, A. J. Sánchez, Hybrid nonlinear MPC of a solar cooling plant, *Energies*, Vol. 12, Issue 14, 2019, 2723.

[13]. E. F. Camacho, A. J. Gallego, A. J. Sánchez, M. Berenguel, Incremental state-space model predictive control of a Fresnel solar collector field, *Energies*, Vol. 12, Issue 1, 2019, 3.

[14]. E. F. Camacho, F. R. Rubio, M. Berenguel, L. Valenzuela, A survey on control schemes for distributed solar collector fields. Part I: Modeling and basic control approaches, *Solar Energy*, Vol. 81, 2007, pp. 1240-1251.

[15]. E. F. Camacho, F. R. Rubio, M. Berenguel, L. Valenzuela, A survey on control schemes for distributed solar collector fields. Part II: Advanced control approaches, *Solar Energy*, Vol. 81, 2007, pp. 1252-1272.

[16]. E. F. Camacho, T. Samad, M. Garcia-Sanz, I. Hiskens. Control for Renewable Energy and Smart Grids, Technical Report, *IEEE Control Systems Society*, 2011.

[17]. E. F. Camacho, M. Berenguel, F. R. Rubio, D. Martnez, Control of Solar Energy Systems, *Springer-Verlag*, 2012.

[18]. R. Carmona, Analysis, modeling and control of a distributed solar collector field with a one-axis tracking system, PhD Thesis, *Universidad de Sevilla*, 1985.

[19]. M. Chilali, P. Gahinet, H_∞ design with pole placement constraints: An LMI approach, *IEEE Transactions on Automatic Control*, Vol. 41, 1996, pp. 358-367.

[20]. A. J. Gallego, E. F. Camacho, Adaptative state-space model predictive control of a parabolic-trough field, *Control Engineering Practice*, Vol. 20, Issue 9, 2012, pp. 904-911.

[21]. A. J. Gallego, E. F. Camacho, Estimation of effective solar irradiation using an unscented Kalman filter in a parabolic-trough field, *Solar Energy*, Vol. 86, 2012, pp. 3512-3518.

[22]. A. J. Gallego, F. Fele, E. F. Camacho, L. J. Yebra. Observer-based model predictive control of a solar trough plant, *Solar Energy*, Vol. 97, 2013, pp. 426-435.

[23]. A. J. Gallego, G. M. Merello, M. Berenguel, E. F. Camacho, Gain-scheduling model predictive control of a Fresnel collector field, *Control Engineering and Practice*, Vol. 82, 2019, pp. 1-13.

[24]. A. J. Gallego, A. Ruz-Pardo, A. Cerezuela-Parish, J. Sánchez Ramos, C. Martn-Macareno, L. F. Cabeza, E. F. Camacho, E. Oró, Mathematical modeling of a PCM storage tank in a solar cooling plant, *Solar Energy*, Vol. 93, 2013, pp. 1-10.

[25]. A. J. Gallego, A. J. Sánchez, M. Berenguel, E. F. Camacho, Adaptive UKF-based model predictive control of a Fresnel collector field, *Journal of Process Control*, Vol. 85, 2020, pp. 76-90.

[26]. A. J. Gallego, M. Macias, F. de Castilla, E. F. Camacho, Mathematical modeling of the Mojave solar plants, *Energies*, Vol. 12, Issue 21, 2019, 4197.

[27]. P. Gil, J. Henriques, A. Cardoso, P. Carvalho, A. Dourado, Affine neural network-based predictive control applied to a distributed solar collector field, *IEEE Transactions on Control Systems Technology*, Vol. 22, Issue 2, 2014, pp. 585-596.

[28]. D. Y. Goswami, F. Kreith, J. F. Kreider, Principles of Solar Engineering, 2nd Ed., *Taylor&Francis*, 2000.

[29]. G. Grossman, M. Wilk, Advanced modular simulation of absorption systems, *International Journal of Refrigeration*, Vol. 17, Issue 4, 1994, pp. 231-244.

[30]. Md. T. Islam, N. Huda, A. B. Abdullah, R. Saidur, A comprehensive review of state of the art concentrating solar power (CSP) technologies: Current status and research trends, *Renewable and Sustainable Energy Reviews*, Vol. 91, 2018, pp. 987-1018.

[31]. M. Karamali, M. Khodabandeh, A distributed solar collector field temperature profile control, estimation using inlet oil temperature and

radiation estimates based on iterative extended Kalman filter, *Renewable Energy*, Vol. 101, 2017, pp. 144-155.
[32]. M. N. Karimi, A. Ahmad, S. Aman, M. D. Jamshed-Khan, A review paper on Vapor absorption system working on LiBr/H_2O, *International Research Journal of Engineering and Technology*, Vol. 5, 2018, pp. 857-864.
[33]. B. Khoukhi, M. Tadjine, M. S. Boucherit, Nonlinear continuous-time generalized predictive control of solar power plant, *International Journal for Simulation and Multidisciplinary Design Optimization*, Vol. 6, 2015, A3.
[34]. D. S. Kima, C. A. Infante-Ferreira, Solar refrigeration options a state-of-the-art review, *International Journal of Refrigeration*, Vol. 31, 2008, pp. 3-15.
[35]. F. Kreith, R. M. Manglik, M. S. Bohn, Principles of Heat Transfer, 7th Ed., *Cengage Learning*, 2011.
[36]. J. M. Lemos, R. Neves-Silva, J. M. Igreja, Adaptive Control of Solar Energy Collector Systems, *Springer-Verlag*, 2014.
[37]. L. Li, C. Hua, H. Yang, A new adaptive unscented Kalman filter based on covariance matching technique, in *Proceedings of the International Conference on Mechatronics and Control (ICMC'14)*, 2014, pp. 1308-1313.
[38]. V. J. Lunardini, Heat Transfer in Cold Climates, *Van Nostrand Reinhold Company*, 1981.
[39]. R. Meligy, M. Rady, A. A El-Samahy, W. Mohamed, F. Paredes, F. Montagnino, Simulation and control of linear fresnel reflector solar plant, *International Journal of Renewable Energy Research*, Vol. 9, 2019, pp. 804-818.
[40]. P. Menchinelli, A. Bemporad, Hybrid model predictive control of a solar air conditioning plant, *European Journal of Control*, Vol. 14, Issue 6, 2008, pp. 501-515.
[41]. M. M. Mokhtar, Control of solar thermal linear Fresnel collector plants in single phase and direct steam generation modes, PhD Thesis, *Institut fur Neutronenphysik und Reaktortechnik (INR)*, Germany, 2019.
[42]. G. F. Naterer, Heat Transfer in Single and Multiphase Systems, *CRC Press*, 2002.
[43]. M. Pasamontes, J. D. Álvarez, J. L. Guzmán, M. Berenguel, Hybrid modeling of a solar cooling system, *IFAC Proceedings Volumes*, Vol. 42, 2009, pp. 26-31.
[44]. M. Pasamontes, J. D. Álvarez, J. L. Guzmán, M. Berenguel, E. F. Camacho, Hybrid modeling of a solar-thermal heating facility, *Solar Energy*, Vol. 97, 2013, pp. 577-590.
[45]. G. Pin, M. Falchetta, G. Fenu, Modeling and control of concentrating solar power systems: a discrete-time adaptative scheme for temperature control in molten-salt solar collector-fields, in Solar Collectors: Energy Conservation, Design and Applications, Series: Renewable Energy: Research, Development and Policies, *Nova Publishers*, 2009, pp. 15-39.

[46]. G. Pin, M.Falchetta, G. Fenu, Adaptative time-warped control of molten salt distributed collector solar fields, *Control Engineering and Practice*, Vol. 16, 2007, pp. 813-823.
[47]. B. Prasartkaew, Mathematical modeling of an absorption chiller system energized by a hybrid thermal system: Model validation, *Energy Procedia*, Vol. 34, 2013, pp. 159-172.
[48]. J. B Rawlings, D. Q. Mayne, Model Predictive Control: Theory and Design, *Nob Hill Publishing LLC*, 2009.
[49]. M. Robledo, J. M. Escano, A. Núnez, C. Bordons, E. F. Camacho, Development and experimental validation of a dynamic model for a Fresnel solar collector, in *Proceedings of the 18th IFAC World Congress*, 2011, pp. 483-488.
[50]. L. Roca, J. L. Guzmán, J. E. Normey-Rico, M. Berenguel, L. Yebra, Robust constrained predictive feedback linearization controller in a solar desalination plant collector field, *Control Engineering Practice*, Vol. 17, Issue 9, 2009, pp. 1076-1088.
[51]. A. Ruz-Pardo, J. M. Salmerón, A. Cerezuela-Parish, A. Gil, S. Álvarez, L. F. Cabeza, Numerical simulation of a thermal energy storage system with PCM in a shell and tube tank, in *Proceedings of the 12th International Conference on Energy Storage*, Innostock, Leida, 16th-18th May, 2012.
[52]. F. R. Rubio, E. F. Camacho, M. Berenguel, Control de campos de colectores solares, *RIAI*, Vol. 3, Issue 4, 2006, pp. 26-45.
[53]. A. Sebastián, R. Abbas, M. Valdés, J. Casanova, Innovative thermal storage strategies for Fresnel-based concentrating solar plants with East-West orientation, *Applied Energy*, Vol. 230, 2018, pp. 983-996.
[54]. SolarPaces, https://solarpaces.nrel.gov/by-technology/linear-fresnel-reflector
[55]. C. Sonntag, H. Ding, S. Engell, Supervisory control of a solar air conditioning plant with hybrid dynamics, *European Journal of Control*, Vol. 14, Issue 6, 2008, pp. 451-463.
[56]. M. Spoladore, E. F. Camacho, M. E. Valcher, Distributed parameters dynamic model of a solar Fresnel collector field, in *Proceedings of the IFAC 18th World Congress*, 2011, pp. 14784-14790.
[57]. Y. Wang, Z. Qiu, X. Qu, An improved unscented Kalman Filter for discrete nonlinear systems with random parameters, *Discrete Dynamics in Nature and Society*, Vol. 2017, 2017, 7905690.
[58]. K. Witheephanich, J. M. Escano, C. Bordóns, Control strategies of a solar cooling plant with Fresnel collector: A case study, in *Proceedings of the International Electrical Engineering Congress (IEEECON'14)*, Chonburi, Thailand, 2014, pp. 1-4.
[59]. K. Witheephanich, J. M. Escano, A. J. Gallego, E. F. Camacho, Pressurized water temperature of a Fresnel collector field type cooling system using explicit model predictive control, in *Proceedings of the IASTED Conference*, Thailand, 2013, pp. 10-12.
[60]. L. Xian-Juan, D. Hai-Ying, Application research of sliding mode predictive control based on feedforward compensation in solar thermal

power generation heat collecting system, *International Journal of Hybrid Information Technology*, Vol. 9, Issue 3, 2016, pp. 211-220.
[61]. D. Zambrano, C. Bordons, W. Garcia-Gabin, E. F. Camacho, A solar cooling plant: a benchmark for hybrid systems control, in *Proceedings of the 2nd IFAC Conference on Analysis and Design of Hybrid Systems (ADHS'06)*, 2006, pp. 199-204.
[62]. D. Zambrano, C. Bordons, W. Garcia-Gabin, E. F. Camacho, Model development and validation of a solar cooling plant, *International Journal of Refrigeration*, Vol. 31, 2008, pp. 315-327.
[63]. D. Zambrano, Modelado y control predictivo hbrido de una planta de refrigeración solar, PhD Thesis, *Escuela Superior de Ingenieros de Sevilla*, 2007.
[64]. Y. Zhou, C. Zhang, Y. Zhang, J. Zhang, A new adaptive square-root unscented Kalman filter for nonlinear systems with additive noise, *International Journal of Aerospace Engineering*, Vol. 2015, 2015, 381478.